BIOCHEMISTRY
including biophysical chemistry & molecular biology

Article

pubs.acs.org/biochemistry

Characterization of the Second Ion-Binding Site in the G Domain of H-Ras

Casey O'Connor[†,‡] and Evgenii L. Kovrigin*[,‡]

[†]Biochemistry Department, Medical College of Wisconsin, 8701 Watertown Plank Road, Milwaukee, Wisconsin 53226, United States
[‡]Chemistry Department, Marquette University, P.O. Box 1881, Milwaukee, Wisconsin 53201, United States

Supporting Information

ABSTRACT: Ras is a small monomeric GTPase acting as molecular switch in multiple cellular processes. The N-terminal G domain of Ras binds GTP or GDP accompanied by a magnesium ion, which is strictly required for GTPase activity and performs a structural role. Another ion-binding site on the opposite face of the G domain has been recently observed to specifically associate with calcium acetate in the crystal [Buhrman, G., et al. (2010) *Proc. Natl. Aacd. Sci. U.S.A. 107*, 4931−4936]. In this article, we report thermodynamic measurements of the affinity and specificity of the remote ion-binding site in H-Ras as observed in solution. Using $^{15}N-^{1}H$ nuclear magnetic resonance spectroscopy, we determined that, in contrast to the crystalline state, the remote site in solution is specific for a divalent cation, binding both calcium and magnesium with anions playing a minimal role. The affinity of the remote site for divalent cations is in the low millimolar range and remarkably different for GDP- and GppNHp-bound forms of the G domain, indicating that the GTP-binding pocket and the remote site are allosterically coupled through the distance of more than 25 Å. Considering that the remote site is oriented toward the membrane surface in vivo, we hypothesize that its cognate biological ligand might be a positively charged group extending from a lipid or an integral membrane protein.

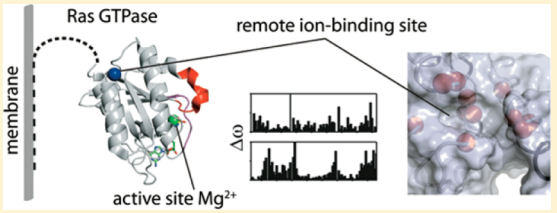

Ras is a prototypical member of a superfamily of small monomeric GTPases that function as molecular switches in a multitude of cellular processes.[1] The switchlike behavior of these proteins is based on distinct conformations observed in GTP-bound ("on", active) or GDP-bound ("off", inactive) states. Ras is kinetically trapped in both end states of a switch, in the active conformation bound with GTP because of low intrinsic GTPase activity and in the inactive conformation because of the extremely slow release of the reaction product, GDP.[2,3] The switch is "flipped" by the action of specific catalysts accelerating these processes, GEFs and GAPs.[4] Numerous downstream effectors recognize the GTP-bound conformation of the effector interface of Ras (switches I and II) and become activated upon binding.[1,5]

Ras consists of a well-folded N-terminal G domain linked with an unstructured C-terminal hypervariable region (HVR) of 22 or 23 amino acids, which is responsible for the specific localization of Ras at the membrane surface[6] (Figure 1). It has recently been proposed that the G domain and HVR do not function completely independently as was once believed but, instead, exhibit a degree of allosteric coupling.[7−11]

The effector interface has a deep cleft flanked by switch I (residues 32−38), which accommodates a GTP or GDP and a structural magnesium ion (Figure 1). The magnesium ion is hexacoordinated by oxygen atoms of β- and γ-phosphates as well as hydroxyls of S17 and T35 and two conserved water molecules.[13] The presence of magnesium is an absolute requirement for both intrinsic and GAP-catalyzed GTPase activity.[14] The ternary complex of Ras with guanine nucleotide and magnesium ion is very stable and characterized by picomolar dissociation constants for nucleotides (in the presence of millimolar magnesium) as well as a low micromolar dissociation constant for magnesium itself.[14−16] Recently, Buhrman and co-workers described the second ion-binding pocket in the G domain of H-Ras·GppNHp as being more than 25 Å from the GTPase active site.[12] In their X-ray diffraction study, the novel ion-binding site was observed to be specific for calcium acetate with the acetate anion buried underneath the calcium cation. Buhrman and co-authors hypothesized that the $Ca^{2+}\cdot CH_3COO^-$ ion pair mimics a yet unknown biological ligand and, in the follow-up paper, obtained evidence that the natural ligand, interacting with this remote site, might be present in the native environment of Ras in the NIH 3T3 cell line.[17]

Intrigued by this discovery of a remote binding site in the G domain, we undertook a solution NMR study to further define its structural and thermodynamic parameters. In the absence of knowledge of a cognate biological ligand, we utilized calcium, magnesium, and sodium salts to probe the specificity and binding affinity of the site in the H-Ras G domain (residues 1−166) complexed with GDP or the GTP mimic GppNHp. The remote site was found to specifically bind divalent cations with millimolar affinity in solution yet not discriminate between calcium and magnesium. It is remarkable that the ions

Received: September 25, 2012
Revised: November 13, 2012
Published: November 13, 2012

   dx.doi.org/10.1021/bi301304g | *Biochemistry* 2012, 51, 9638−9646

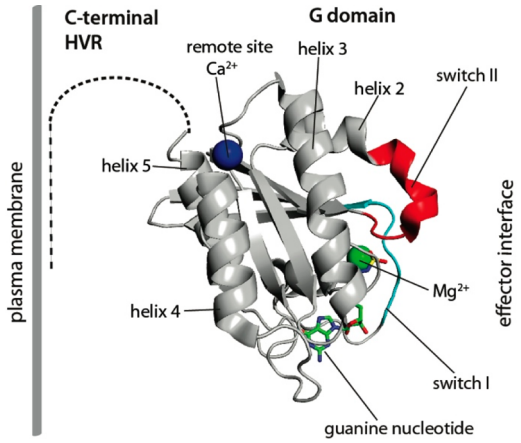

Figure 1. Schematic of the Ras GTPase showing general structural features as well as the remote ion-binding site near a C-terminal region. The structure of the G domain of H-Ras (residues 1−166) complexed with GppNHp, Mg^{2+}, and Ca^{2+} (Protein Data Bank entry 3K8Y[12]) is shown as a cartoon with magnesium (green sphere) in the GTPase active site and calcium (blue sphere) in the remote site. The GTP mimic, GppNHp, is shown in a stick representation with oxygen, nitrogen, and carbon atoms colored red, blue, and green, respectively. Switch regions are depicted as cyan (switch I) and red (switch II) cartoons. The C-terminal hypervariable region (HVR) is schematically represented as a dashed line tethering the G domain to the membrane surface (drawing not to scale).

interacted stronger with the remote site in the GDP form of the G domain than in the GTP-mimicked form, despite the 25 Å distance from the nucleotide-binding pocket. Structural analysis of the pocket reveals its flexible nature, thus accounting for weak interactions with small ions and indicating that the site may be adaptable to accommodate a larger natural ligand.

MATERIALS AND METHODS

The G domain of H-Ras residues 1−166 was expressed in *Escherichia coli* as inclusion bodies, isolated, refolded, and purified as described previously[18] with little modification. After ion-exchange and size-exclusion chromatography steps, the protein purity was greater than 95% (judged by sodium dodecyl sulfate−polyacrylamide gel electrophoresis).

Nucleotide exchange was performed as described previously[18] in the presence of GppNHp (Sigma) at a 2:1 molar ratio of nucleotide to protein. Shrimp alkaline phosphatase (Fermentas) was added (10 units) to hydrolyze released GDP molecules and drive the exchange reaction to completion. Exchange was allowed to proceed for 120 min at 20 °C. The obtained Ras·GppNHp complex was extensively dialyzed against "NMR buffer" containing 10 mM TRIS (pH 7.2), 1 mM DTT, 10 mM NaCl, 10 μM $MgCl_2$, and 0.01% NaN_3. The equilibrium concentration of magnesium in the buffer has been chosen to significantly exceed the dissociation constant of the magnesium ion in the GTPase active site (2.8 μM in the H-Ras·GDP complex[14]). Following dialysis, the protein was concentrated using centrifugal filters (Amicon) with a molecular mass cutoff of 3000 kDa. The final concentration of Ras in NMR samples ranged from 0.4 to 1.0 mM.

A typical titration series included eight points corresponding to different molar ratios of ligand to protein in a sample (L/P) equal to 0, 0.5, 1, 2, 3, 5, 10, and 20. To prepare these solutions most accurately, we started with two protein solutions: A, without a ligand (L/P = 0), and B, with the ligand added to create an L/P of 20. These two solutions correspond to the starting and ending points of the titration series. To prepare intermediate titration points, we added solution B in small aliquots to solution A in the NMR tube. Addition of the last remaining volume of solution B to solution A created the final titration point with an L/P of 10. In this titration design, one avoids a pH drift during titrations because pH values of both solutions A and B are made equal. The protein concentration also remains constant, allowing for equal sensitivity throughout the titration series. Measurement of sequential aliquots of solution B was performed using an eVol NMR Edition precision electronic syringe (SGE Analytical Science).

For $^1H-^{15}N$ HSQC experiments, ^{15}N-labeled Ras samples were placed in a 3 mm tube with a final volume of 200 μL or a 5 mm tube with a final volume of 500 μL. Experiments were performed at 293.15 K using Bruker Avance II and Varian VNMR-S spectrometers operating at a magnetic field strength of 14.1 T and equipped with cryogenic probes. Spectra were processed with NMRPipe[19] and visualized with Sparky.[20] NMR signal assignment for the Ras·GDP complex has been performed following the protocol described previously[21] and deposited in the BioMagResBank (entry 18479). NMR assignments for the Ras·GppNHp complex were taken from our earlier publication.[21]

For chemical shift perturbation maps, to achieve maximal resolution, we used a shifted sine-bell apodization function. To prepare spectral data for analysis of NMR line shapes, we employed an exponential apodization function. Chemical shift perturbations were calculated as a weighted average of chemical shift changes in proton and nitrogen dimensions according to the equation[22]

$$\Delta\omega = \sqrt{(\omega_H{}^2 + \omega_N{}^2/25)/2}$$

To identify peaks affected by ligand binding, the chemical shift perturbations were plotted as a histogram (Figure S1 of the Supporting Information) showing the observed number of peaks experiencing the particular chemical shift change. Perturbations of chemical shifts due to nonspecific effects (overall solvent effect and/or sample temperature fluctuations) were observed as a narrow distribution centered around 0.008 ppm. This "random" distribution quickly falls off; very few residues are expected to show large chemical shift changes. Therefore, when a significant number of residues were observed experiencing large $\Delta\omega$ values, this was interpreted as a signature of specific binding. Mapping of chemical shift perturbations on Ras crystal structures was performed using the PyMOL molecular visualization system (Schrödinger).

Extraction of one-dimensional line shapes for fitting to determine binding affinity was performed with the custom Sparky extension, *IDAP 1D NMR* (E. L. Kovrigin, unpublished work), followed by fitting using Integrative Data Analysis Platform (IDAP).[23] In brief, NMR data are processed with an exponential apodization function to obtain Lorentzian line shapes in the frequency domain.[24] The one-dimensional NMR line shapes, extracted from two-dimensional HSQC planes, are combined in one data set as a function of an increasing ligand:protein ratio (L/P). The position and line width of the resonance at L/P = 0 are determined by fitting with the Lorentzian line shape function. Theoretical NMR line shapes for the two-state binding model are simulated using Bloch−McConnell equations[25] as a function of L/P and fit to the experimental data to obtain the dissociation constant, off rate

dx.doi.org/10.1021/bi301304g | *Biochemistry* 2012, 51, 9638−9646

constant, frequency, and line width of the fully saturated resonance, and an intensity scaling factor (see also refs 23, 26, and 27). Fitting parameters were determined individually for each data set followed by global fitting of a superdata set containing spectral series from multiple residues and (where possible) orthogonal frequency dimensions. Monte Carlo simulations were used to estimate the uncertainty of the best-fit parameters. The exchange between free and bound forms of Ras was fast as judged by the observation of continuously shifted peaks with minimal line broadening. Correspondingly, fitting for K_d and k_{off} resulted in well-defined values of the former and poorly defined values for the latter (95% of Monte Carlo results for k_{off} fell between 1500 and 5000 s^{-1}). Therefore, in our analysis of binding affinity, the k_{off} was fixed to a value between 2000 and 3000 s^{-1}, the choice of which did not affect fitting quality or results.

RESULTS

Mapping of Ion-Binding Sites in the Active and Inactive Forms of the Ras G Domain. To probe ionic interactions of the G domain in biologically active and inactive forms, we utilized H-Ras residues 1−166 in a complex with a GTP mimic, GppNHp, or with GDP (in the following text, Ras·GppNHp and Ras·GDP, respectively). The two-dimensional $^1H-^{15}N$ HSQC NMR spectra of isotopically labeled Ras·GppNHp and Ras·GDP samples were acquired in solution at pH 7.2 and 20 °C with calcium acetate added to a final concentration 20 times that of the protein. The ligand addition resulted in significant perturbations of chemical shifts of NH groups of a number of residues. Figure 2A shows representative specific perturbations at residues V109 and I139 upon addition of calcium acetate. The small shift of a cross-peak for E49 is characteristic of an overall solvent effect. Chemical shift perturbations induced by calcium acetate at different residues in Ras·GppNHp and Ras·GDP are summarized in panels B and C of Figure 2, respectively. Among all assigned and sufficiently resolved NH cross-peaks in Ras·GppNHp, addition of calcium acetate perturbed the position of signals for residues Y4, K16, F28, L79, V109, V112, G138, and I139. In Ras·GDP, significant perturbations were induced at residues T2, N26, T58, L79, D92, I93, H95, R97, V109, M111, V112, G138, I139, L159, I163, R165, and H166. Figure 3 depicts localization of these sites in the structural models of Ras·GppNHp and Ras·GDP.

Determination of the Specificity of the Ionic Interactions. To help identify individual contributions of cations and anions to binding, we performed titrations of Ras·GppNHp and Ras·GDP with sodium acetate, calcium chloride, and magnesium chloride. The titration with calcium chloride that is shown in Figure 4A was most similar to the titration with calcium acetate shown in panels B and C of Figure 2. Magnesium chloride produced the same pattern of chemical shift perturbations (Figure 4B) with a smaller overall amplitude, while addition of a 20-fold molar excess of sodium acetate did not induce significant shifts in NH cross-peaks (Figure 4C), indicating a lack of specific interaction of the acetate ion.

Affinity of Ionic Interactions in GTP-Mimicking and GDP Forms of Ras. To determine binding affinities, we extracted one-dimensional line shapes from a series of two-dimensional HSQC spectra (Figure 5A) at multiple ligand:-protein ratios and fit them with Bloch−McConnell equations (Figure 5B). Figure S2 of the Supporting Information additionally illustrates these line shape fitting results in the form of a conventional chemical shift titration curve. We chose the amide NH cross-peaks of G138 and I139 as reporters for the affinity and ligand preferences of the remote ion-binding site because they were sufficiently isolated in all titrations. Results of fitting of these residues as a set are listed in Table 1 for each individual titration.

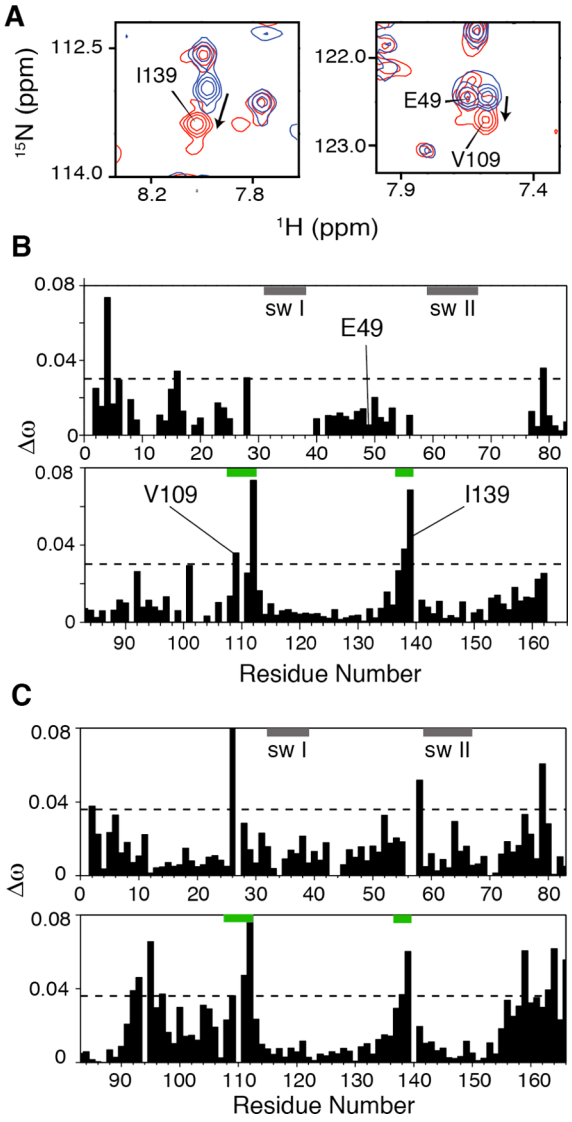

Figure 2. Chemical shift perturbations due to addition of calcium acetate to the G domain of H-Ras(1−166) to a final concentration of 10−20 mM (20-fold molar excess with respect to Ras). (A) Representative HSQC spectral regions demonstrating shifts of cross-peaks upon addition of calcium acetate to Ras·GppNHp (with 10 μM $MgCl_2$ in the background). Blue and red contours represent spectra at the ligand:protein ratios of 0 and 20, respectively. Chemical shift perturbations of amide ^{15}N and ^1H (a combined weight-average value) are shown as bar graphs for all assigned residues in Ras·GppNHp (B) and Ras·GDP (C). The top half of each panel corresponds to the first 83 amino acids, and the bottom half shows the rest of the sequence (residues 84−166). Places where bars are missing correspond to residues with signals broadened or insufficiently resolved for reliable analysis, and also to prolines 34, 110, and 140. Gray horizontal bars indicate locations of switch regions I and II. Green horizontal bars indicate amino acids D108−V112 and Y137−I139 in the remote ion-binding site identified by Buhrman and co-workers.[12] The dashed line represents a cutoff used to identify NH groups with statistically significant perturbations.

dx.doi.org/10.1021/bi301304g | Biochemistry 2012, 51, 9638−9646

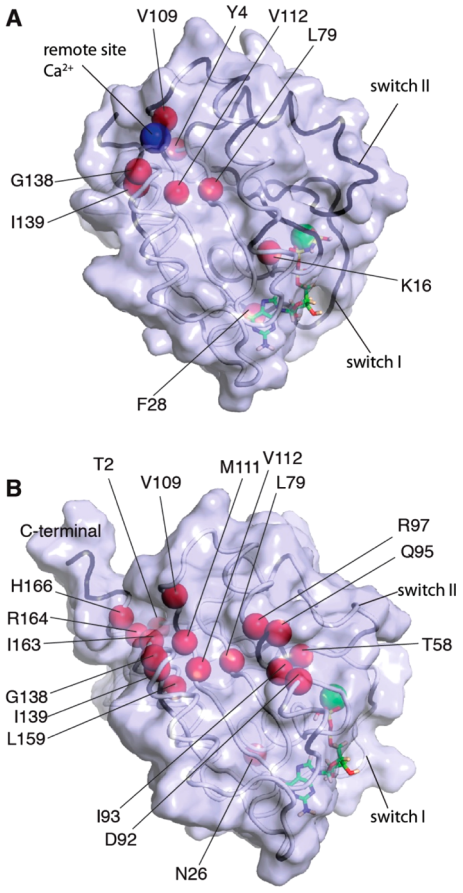

Figure 3. Chemical shift perturbations due to calcium acetate binding at the remote site in Ras·GppNHp (A) and Ras·GDP (B). The G domain is shown in the same orientation as in Figure 1. Red spheres represent amide NH groups with the combined chemical shift perturbation exceeding the cutoff values shown by the dashed lines in panels B and C of Figure 2. The backbone trace is represented as a tube. The black tube corresponds to unassigned regions (regions where the bars are missing in Figure 2). Panel A shows the H-Ras(1−166)·GppNHp·Mg^{2+}·Ca^{2+} model based on the crystal structure of PDB entry 3K8Y[12] with a calcium ion (blue sphere) bound to the remote site. Because the calcium-bound H-Ras·GDP·Mg^{2+} structure is not available, panel B represents titration data mapped onto the H-Ras(1−169)·GDP·Mg^{2+} structural model from PDB entry 1Q21[28] in the same orientation.

It is important to note that these titrations were performed at a low ionic strength, in the presence of 10 mM NaCl, to improve NMR sensitivity. To measure the effect of the physiological ionic strength on the ion binding affinity of the remote site, we performed a titration of Ras·GDP with calcium acetate in the presence of 150 mM NaCl. Because of signal overlap of I139, spectral data for fitting were extracted from both proton and nitrogen spectral dimensions for V109 and G138. The best-fit K_d from the global fitting of all four data sets is given in the bottom row of Table 1. The corresponding chemical shift perturbation map and the representative fitting graph are shown in Figures S3 and S4 of the Supporting Information. Analysis of the ionic strength effect on the dissociation constants revealed that the remote site is likely to carry a charge of −2 [with a 95% confidence interval from −1.7 to −2.7 (see the Supporting Information for details)].

Additionally, binding interactions of the T2 NH group in Ras·GDP with calcium acetate were also evaluated as being representative of perturbations seen at the extreme N-terminus of the G domain at 10 mM NaCl. Global fitting of line shapes extracted from both nitrogen and proton dimensions of the T2 NH cross-peak resulted in a K_d of 3.0 mM with the 95% confidence interval ranging from 2.4 to 3.3 mM.

DISCUSSION

The Second Ion-Binding Site (the "remote site") Exists in Ras·GppNHp and Ras·GDP. This work has been inspired by the crystallographic study of Buhrman and co-workers reporting a remarkable pocket on the C-terminal part of the G domain in H-Ras·GppNHp that specifically bound a calcium acetate ion pair.[12] Our results in Figure 2 indicate that, in solution, chemical shifts of a number of sites in both Ras·GppNHp and Ras·GDP are sensitive to addition of calcium acetate with many significant perturbations localized to the neighborhood of the remote site (indicated by green bars in Figure 2 and seen on a molecular model of the G domain in Figure 3). Therefore, we can conclude that the remote site is present in both active and inactive Ras conformations (GTP-mimicking and GDP forms). Our assignment coverage was significantly better in Ras·GDP, allowing for a more accurate mapping of perturbations in the immediate vicinity of the remote site (Figure 6). Perturbations accurately map out roughly a 5 Å × 10 Å pocket on the rear surface of the G domain at the end of helix 4, flanked by loop 7 and C-terminal helix 5.

It is notable that the ion binding event affects not only residues on the surface of the protein but also residues in the hydrophobic core (L79 and V112) and, in the GDP form, at the more distant helix 3 (D92, I93, Q95, and R97 in Figure 3B). The perturbation of chemical shifts that are deep in a protein structure cannot occur because of direct physical contact with the ligand and is, typically, a signature of a ligand-induced conformational rearrangement that is altering the local magnetic environment of the ^{15}N and ^{1}H nuclear spins.[24] When calcium acetate was found in the remote site in the Ras·GppNHp crystals, Buhrman and co-workers noted a significant shift of helix 3 and ordering of the switch II region (elongation of helix 2).[12] Unfortunately, we cannot comment on the involvement of helix 2 in the proposed allosteric transition in solution because signals from most of helix 2 in Ras·GppNHp in our experiments were broadened beyond detection (indicated by the black coloring of the ribbon in Figure 3A; consistent with an earlier report by Ito and co-workers[29]). However, we did achieve nearly complete signal assignment in the Ras·GDP form, and signals from helix 2 are observable and well-resolved. We did not observe the expected massive perturbations in switch 2 upon addition of calcium acetate (Figure 3B), but it is also not known whether calcium binding to the remote site in Ras·GDP in the crystal should trigger a similar allosteric conformational change.

The Remote Site Is Specific for a Divalent Cation. When the remote site was discovered in 2010, it was found to be strictly specific for the calcium acetate ion pair (not calcium chloride or magnesium acetate).[12] In solution, we observed that both calcium acetate and calcium chloride bind to the remote site (cf. Figures 2B,C and 4A), and magnesium chloride has similar binding properties (Figure 4B). On the contrary, sodium acetate did not interact with the G domain (Figure 4C). These data indicate that it is a divalent cation that makes important interactions with the remote site in the G domain while the role of the anion in defining specificity is relatively

dx.doi.org/10.1021/bi301304g | Biochemistry 2012, 51, 9638−9646

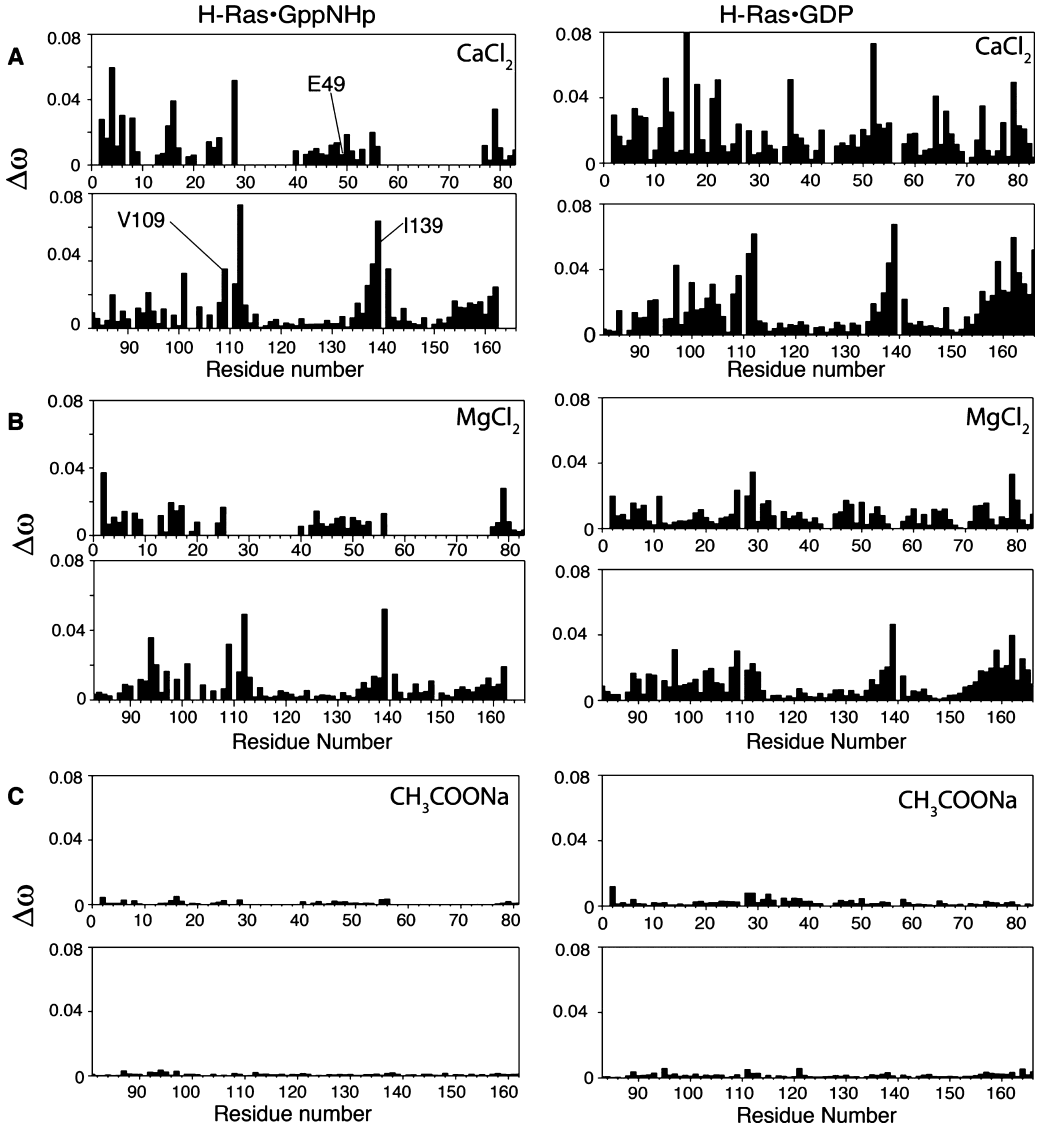

Figure 4. Chemical shift perturbations in Ras·GppNHp (left) and Ras·GDP (right) induced by a 20-fold molar excess of calcium chloride (A), magnesium chloride (B), and sodium acetate (C).

minor. Quantitative analysis of the titrations (Figure 5 and Table 1) revealed millimolar dissociation constants for binding of the divalent cation to the remote site. The titration of Ras·GDP with calcium acetate at the physiological ionic strength showed a moderate 4-fold reduction in binding affinity.

On the basis of measured millimolar dissociation constants of the magnesium and calcium ions, it is likely that binding of these ions by themselves is irrelevant in the biological context. The intracellular concentration of free magnesium in the cytosol of a eukaryotic cell is ~0.5 mM,[30] which is smaller than the K_d values reported in Table 1, implying that the remote site is occupied by magnesium in vivo for only a small fraction of time. The intracellular concentration of calcium ions is even lower, in the 10 nM to 1 μM range, which may increase upon stimulation to only 10 μM,[31] significantly lower than the measured millimolar K_d values. These results support the proposal that the cognate biological ligand must be different from calcium or magnesium[17] but could, possibly, cooperate with them upon binding; therefore, we considered divalent ions in our experiments only as probes of the remote site to reveal its relationship to the rest of the G domain structure.

The Remote Site and the Nucleotide-Binding Pocket Are Allosterically Coupled. Table 1 demonstrates that the exchange of the nucleotide from GppNHp to GDP leads to a statistically significant decrease in the K_d for all three salts: calcium acetate, calcium chloride, and magnesium chloride. In the G domain, the remote site is located more than 25 Å from the nucleotide-binding pocket (Figure 1) and no direct influence of a nucleotide structure on the remote site properties is possible. Therefore, the observed dependence of the remote site affinity upon a particular type of nucleotide bound at the effector interface may serve as clear evidence of the allosteric coupling between opposite faces of the G domain.

We propose that this allosteric coupling is related to the structural rigidity of the G domain as a whole. GppNHp is known to be a relatively weakly binding mimic with a 10-fold lower affinity than GDP.[15] Accordingly, Ras·GppNHp was reported to be more flexible than Ras·GDP; significant exchange broadening was observed at multiple peaks in HSQC spectra of Ras·GppNHp but not Ras·GDP.[29] We also

dx.doi.org/10.1021/bi301304g | *Biochemistry* 2012, 51, 9638−9646

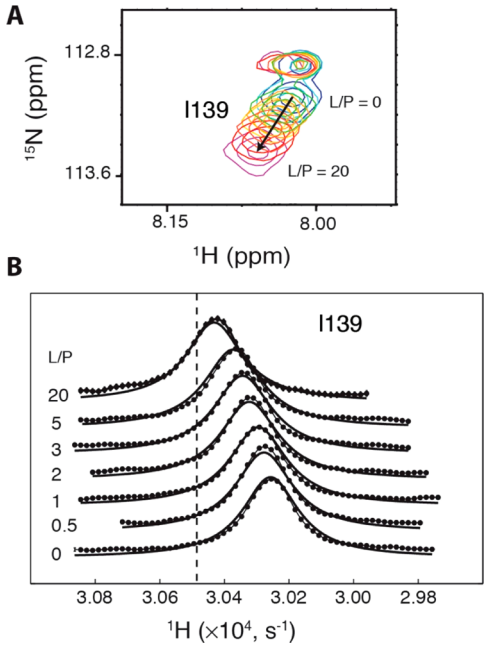

Figure 5. Quantitative analysis of ion titrations. (A) Representative overlay of the amide ^{15}N–^{1}H HSQC spectra corresponding to sequential additions of calcium acetate to H-Ras(1–166)·GDP·Mg^{2+}. A rainbow color scheme is used to show progressive shifting of the I139 resonance. The one-dimensional line shapes extracted from this HSQC series in the proton dimension are shown in panel B. The corresponding ligand:protein molar ratios are indicated next to the traces. Experimental spectral data are given by symbols connected by straight lines (noise root-mean-square deviation was on the order of magnitude of the symbol size); the best-fit results are shown as smooth solid lines. A vertical dashed line indicates the best-fit frequency of a fully saturated resonance.

Table 1. Dissociation Constants, K_d, of the Remote Site Determined via Analysis of NMR Titrations[a]

	K_d (95% confidence interval) (mM)	
	Ras·GppNHp	Ras·GDP
$Ca(CH_3COO)_2$	5.9 (5.4–6.5)	1.5 (1.3–1.8)
$CaCl_2$	4.5 (3.5–4.8)	0.90 (0.89–0.91)
$MgCl_2$	5.4 (4.5–6.9)	1.9 (1.6–2.2)
$Ca(CH_3COO)_2$ at 150 mM NaCl	—	6.3 (5.7–8.3)

[a]All data correspond to 10 mM NaCl in the buffer except where indicated. The results are given as the most likely value of K_d and (in parentheses) the boundaries enclosing 95% of the best-fit results determined via Monte Carlo analysis.

reported an observation of conformational dynamics that encompasses most of the G domain in Ras·GppNHp,[18] indicating that it is flexible on a millisecond time scale. If the G domain is more rigid with GDP than with GppNHp, this increased structural rigidity would reduce the entropic cost of ligand binding at the remote pocket, resulting in the lower K_d values, which we observed in our titration experiments.

Other Sites Interacting with Ions in the G Domain. Examination of panels B and C of Figure 2 and panels A and B of Figure 4 reveals some sites on a protein surface that are distant from both the active site magnesium and the remote site calcium ions yet are quite responsive to addition of the divalent cations. In particular, these are T2 (Ras·GDP with calcium acetate and Ras·GppNHp with magnesium chloride), Y4

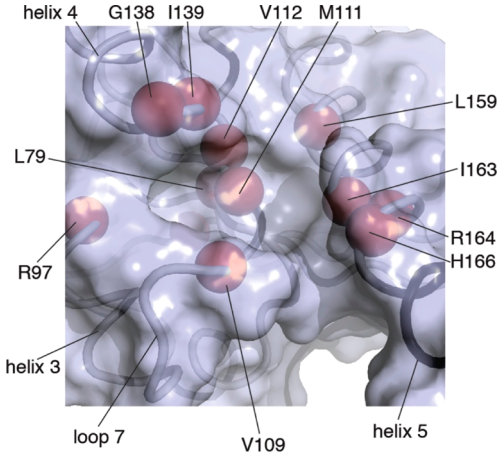

Figure 6. Top view of the remote ion-binding pocket. The amide NH groups significantly perturbed by calcium acetate addition are shown as red spheres. The protein backbone is represented as a ribbon diagram, and the translucent surface shows the remote pocket on the H-Ras·GDP·Mg^{2+} complex modeled using PDB entry 1Q21.

(Ras·GppNHp with calcium acetate and calcium chloride), N26 (Ras·GDP with calcium acetate), and Y28 (Ras·GppNHp with calcium chloride). Inspection of published crystal structures of Ras obtained in the presence of calcium (PDB entries 30IW, 30IV, 30IU, 2RGE, 3L8Z, and 3K8Y) reveals that calcium ions tend to associate with these sites. Their surface location implies weaker affinity, which is indeed the case: for example, the K_d of the T2 site in the titration of Ras·GDP with calcium acetate was determined to be in the range from 2.4 to 3.3 mM, twice as high as that of the remote site in Ras·GDP.

Another site of perturbations with calcium salts is in the vicinity of the magnesium ion in the GTPase active site (Figure 1), residues G12, K16, and A18 and others. These perturbations are consistent with competition for the active site between calcium and magnesium, leading to partial replacement with the former at high calcium:protein molar ratios. Correspondingly, these sites experience minimal perturbations upon addition of magnesium salts.

The Remote Site Is Negatively Charged. A recent crystallographic and cell biological study by Mattos' group presented evidence that the natural ligand for the remote site might exist in a human fibroblast cell line.[17] The identity of this ligand remains unknown, but some insights may be gleaned from consideration of the shape and nature of the binding pocket. The remote site is expected to be negatively charged with the acidic side chains of D107, D108, and E162 forming the outer rim of the binding pocket (Figure 7A). Our analysis of the K_d as a function of ionic strength suggests the effective charge of −2 (from −1.7 to −2.7) at the remote site in the ligand-free form and −1 (from −0.7 to −1.7) after binding the ion pair. The charged nature of the remote site was a likely reason why it has not been highlighted in two recent small molecule screening studies: Multiple Solvent Crystal Structures by Mattos' group[32] and screening of a 3300-compound library against H-Ras at Genetech.[33] Both approaches used compounds biased toward noncharged moieties that were aimed at detection of nonpolar binding sites. The only screening approach that reliably determined the remote site location was an in silico fragment-based screening as implemented in FTMap,[34] when a cluster of molecular fragments was reliably fit into this pocket.[32] Electrostatic interactions of metal chelates

dx.doi.org/10.1021/bi301304g | Biochemistry 2012, 51, 9638–9646

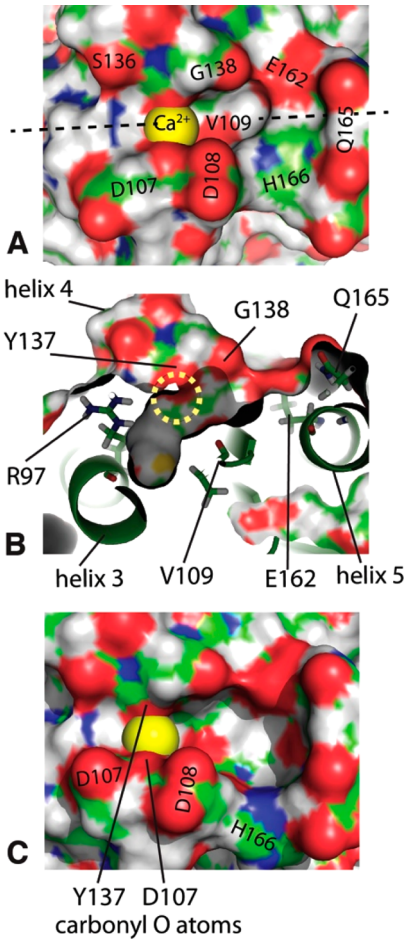

Figure 7. Composition of the remote binding pocket in the H-Ras G domain (residues 1−166). Panel A shows a surface view of the structural model of Protein Data Bank entry 3K8Y. Oxygen atoms are colored red, nitrogens blue, carbons green, and hydrogens white. The bound calcium ion is a yellow sphere. A dashed line indicates a position of an orthogonal plane that corresponds to a cross section of the pocket shown in panel B. The position of the calcium ion is indicated with a yellow dashed circle. The counterion, acetate, bound underneath the calcium is not shown. Panel C is a view of a pocket in another calcium-bound structure, PDB entry 3LBH, demonstrating the alternative orientation of the H166 side chain. The carbonyl oxygen atoms of D107 and Y137 coordinating the calcium ion are labeled.

with the negatively charged side chains of loop 7 were also detected by Rosnizeck et al., who reported the stable association of Cu^{2+} and Zn^{2+} cyclens outside of the binding pocket of the remote site.[35]

The Binding Pocket Is Relatively Deep and Flexible. Figure 7B depicts a cross section of the remote site passing through the calcium ion. The pocket extends into the interior of the protein with the inner part accommodating an acetate anion in the structures of PDB entries 3K8Y and 3LBH (likely, also accommodating the chloride ion in titrations with chloride salts). Because of the lack of perturbations that was documented with sodium acetate (Figure 4C), the anion appears to occupy the pocket only in the presence of the divalent cation (which is in accord with the predicted negative charge of the remote site).

The pocket is flanked by loop 7 (S106, D107, and D108), which provides flexibility to the pocket shape, and C-terminal helix 5 with H166 serving as another "adjustable" wall (cf. panels A and C in Figure 7). Visual examination of the pocket shape in multiple crystal structures (Figure S5 of the Supporting Information) further supports the idea that this is an adaptable binding site. It is curious that the negatively charged loop 7 and H166 also provided a binding surface for the Cu^{2+} and Zn^{2+} cyclens, which were binding outside of the remote site.[35]

The Likelihood of Binding Interactions Is Increased Because of the Proximity to the Membrane. In the cell, Ras is always tethered to the membrane via the flexible C-terminus that extends from helix 5 directly beyond the remote site (schematically depicted in Figure 1).[1,36] Therefore, this face of the G domain is necessarily membrane-oriented, making it possible for a membrane-bound ligand (a lipid or a membrane protein) to access the site. Having both binding partners (the ligand and Ras itself) tethered to the membrane reduces the entropy loss upon binding; therefore, even relatively weak electrostatic and van der Waals interactions may result in a significant Gibbs energy increase and higher binding affinity.

Another way of expressing this idea of a higher binding affinity expected in the membrane-associated system is to consider effective concentrations of the binding partners. When both binding partners are bound to a membrane, they no longer undergo three-dimensional diffusion but diffuse only in two dimensions instead. It was estimated that the reduction of dimensionality may increase effective concentrations of binding partners by a factor of 1000.[37,38] Therefore, while calcium and magnesium salts utilized to probe the binding properties of the remote site in solution showed low affinities, the cognate membrane-bound ligand might interact much stronger with the remote site in Ras associated with a membrane surface.

■ CONCLUSIONS

In this work, we analyzed the thermodynamic and structural properties of the remote ion-binding pocket in the G domain of H-Ras. We observed that this site is specific for divalent cations and allosterically coupled to the classical nucleotide-binding pocket. On the basis of this evidence, we hypothesize that the remote site may be a part of yet another mechanism for regulation of Ras signaling by membrane-bound positively charged ligands.

■ ASSOCIATED CONTENT

Supporting Information

Estimation of the charge of the remote site, chemical shift perturbation map and fitting results for titrations at 150 mM NaCl, images of the remote site and its cross section in different crystal structures, and a representative histogram of chemical shift changes. This material is available free of charge via the Internet at http://pubs.acs.org.

■ AUTHOR INFORMATION

Corresponding Author

*Chemistry Department, Marquette University, P.O. Box 1881, Milwaukee, WI 53201. Phone: (414) 288-7859. E-mail: evgueni.kovriguine@marquette.edu.

Author Contributions

The manuscript was written through contributions of all authors. All authors have given approval to the final version of the manuscript.

Funding

E.L.K. acknowledges Program Development funds from the Medical College of Wisconsin and from Marquette University.

Notes

The authors declare no competing financial interest.

■ ACKNOWLEDGMENTS

We acknowledge Dr. Brian Volkman and Dr. Vaughn Jackson for critical reading of the manuscript and Drs. Jung-Ja Kim, Jimmy Feix, and James Kincaid for helpful discussions.

■ ABBREVIATIONS

GDP, guanine diphosphate; GppNHp, guanosine 5′-[β,γ-imido]triphosphate; NMR, nuclear magnetic resonance; HSQC, heteronuclear single-quantum coherence; PDB, Protein Data Bank.

■ REFERENCES

(1) Wittinghofer, A., and Vetter, I. R. (2011) Structure-Function Relationships of the G Domain, a Canonical Switch Motif. In *Annual Reviews of Biochemistry* (Kornberg, R. D., Raetz, C. R. H., Rothman, J. E., and Thorner, J. W., Eds.) pp 943−971, Annual Reviews, Palo Alto, CA.

(2) John, J., Schlichting, I., Schiltz, E., Rosch, P., and Wittinghofer, A. (1989) C-Terminal Truncation of P21h Preserves Crucial Kinetic and Structural Properties. *J. Biol. Chem. 264*, 13086−13092.

(3) Li, G., and Zhang, X. C. (2004) GTP Hydrolysis Mechanism of Ras-like GTPases. *J. Mol. Biol. 340*, 921−932.

(4) Bos, J. L., Rehmann, H., and Wittinghofer, A. (2007) GEFs and GAPs: Critical elements in the control of small G proteins. *Cell 129*, 865−877.

(5) Malumbres, M., and Barbacid, M. (2003) RAS oncogenes: The first 30 years. *Nat. Rev. Cancer 3*, 459−465.

(6) Prior, I. A., and Hancock, J. F. (2012) Ras trafficking, localization and compartmentalized signalling. *Semin. Cell Dev. Biol. 23*, 145−153.

(7) Thapar, R., Williams, J. G., and Campbell, S. L. (2004) NMR Characterization of Full-length Farnesylated and Non-farnesylated H-Ras and its Implications for Raf Activation. *J. Mol. Biol. 343*, 1391−1408.

(8) Gorfe, A. A., Hanzal-Bayer, M., Abankwa, D., Hancock, J. F., and McCammon, J. A. (2007) Structure and Dynamics of the Full-Length Lipid-Modified H-Ras Protein in a 1,2-Dimyristoylglycero-3-phosphocholine Bilayer. *J. Med. Chem. 50*, 674−684.

(9) Abankwa, D., Hanzal-Bayer, M., Ariotti, N., Plowman, S. J., Gorfe, A. A., Parton, R. G., McCammon, J. A., and Hancock, J. F. (2008) A novel switch region regulates H-ras membrane orientation and signal output. *EMBO J. 27*, 727−735.

(10) Edreira, M. M., Li, S., Hochbaum, D., Wong, S., Gorfe, A. A., Ribeiro-Neto, F., Woods, V. L., and Altschuler, D. L. (2009) Phosphorylation-induced Conformational Changes in Rap1b: Allosteric Effects on Switch Domains and Effector Loop. *J. Biol. Chem. 284*, 27480−27486.

(11) Abankwa, D., Gorfe, A. A., Inder, K., and Hancock, J. F. (2010) Ras membrane orientation and nanodomain localization generate isoform diversity. *Proc. Natl. Acad. Sci. U.S.A. 107*, 1130−1135.

(12) Buhrman, G., Holzapfel, G., Fetics, S., and Mattos, C. (2010) Allosteric modulation of Ras positions Q61 for a direct role in catalysis. *Proc. Natl. Acad. Sci. U.S.A. 107*, 4931−4936.

(13) Pai, E., Krengel, U., Petsko, G., Goody, R., Kabsch, W., and Wittinghofer, A. (1990) Refined crystal structure of the triphosphate conformation of H-ras p21 at 1.35 Å resolution: Implications for the mechanism of GTP hydrolysis. *EMBO J. 9*, 2351−2359.

(14) John, J., Rensland, H., Schlichting, I., Vetter, I., Borasio, G. D., Goody, R. S., and Wittinghofer, A. (1993) Kinetic and structural analysis of the Mg^{2+}-binding site of the guanine nucleotide-binding protein p21H-ras. *J. Biol. Chem. 268*, 923−929.

(15) Scherer, A., John, J., Linke, R., Goody, R. S., Wittinghofer, A., Pai, E. F., and Holmes, K. C. (1989) Crystallization and Preliminary X-ray Analysis of the Human c-H-ras-Oncogene Product p21 Complexed with GTP Analogues. *J. Mol. Biol. 206*, 257−259.

(16) John, J., Sohmen, R., Feuerstein, J., Linke, R., Wittinghofer, A., and Goody, R. (1990) Kinetics of interaction of nucleotides with nucleotide-free H-ras p21. *Biochemistry 29*, 6058−6065.

(17) Buhrman, G., Kumar, V. S. S., Cirit, M., Haugh, J. M., and Mattos, C. (2011) Allosteric Modulation of Ras-GTP Is Linked to Signal Transduction through RAF Kinase. *J. Biol. Chem. 286*, 3323−3331.

(18) O'Connor, C., and Kovrigin, E. L. (2008) Global conformational dynamics in Ras. *Biochemistry 47*, 10244−10246.

(19) Delaglio, F., Grzesiek, S., Vuister, G. W., Zhu, G., Pfeifer, J., and Bax, A. (1995) NMRPipe: A multidimensional spectral processing system based on UNIX pipes. *J. Biomol. NMR 6*, 277−293.

(20) Goddard, T. D., and Kneller, D. G. (2010) *SPARKY 3*, University of California, San Francisco. http://www.cgl.ucsf.edu/home/sparky/, accessed 11/2012.

(21) O'Connor, C., and Kovrigin, E. L. (2012) Assignments of backbone ^{1}H, ^{13}C and ^{15}N resonances in H-Ras (1−166) complexed with GppNHp at physiological pH. *Biomol. NMR Assignments 6*, 91−93.

(22) Grzesiek, S., Stahl, S. J., Wingfield, P. T., and Bax, A. (1996) The CD4 Determinant for Downregulation by HIV-1 Nef Directly Binds to Nef. Mapping of the Nef Binding Surface by NMR. *Biochemistry 35*, 10256−10261.

(23) Kovrigin, E. L. (2012) NMR line shapes and multi-state binding equilibria. *J. Biomol. NMR 53*, 257−270.

(24) Cavanaugh, J., Fairbrother, W. J., Palmer, A. G., III, and Skelton, N. J. (2006) *Protein NMR Spectroscopy: Principles and Practice*, Academic Press, New York.

(25) McConnell, H. (1958) Reaction rates by nuclear magnetic resonance. *J. Chem. Phys. 28*, 430−431.

(26) Kovrigin, E. L., and Loria, J. P. (2006) Enzyme dynamics along the reaction coordinate: Critical role of a conserved residue. *Biochemistry 45*, 2636−2647.

(27) Greenwood, A., Rogals, M., De, S., Lu, K., Kovrigin, E., and Nicholson, L. (2011) Complete determination of the Pin1 catalytic domain thermodynamic cycle by NMR lineshape analysis. *J. Biomol. NMR 51*, 21−34.

(28) Tong, L. A., de Vos, A. M., Milburn, M. V., and Kim, S. H. (1991) Crystal structures at 2.2 Å resolution of the catalytic domains of normal ras protein and an oncogenic mutant complexed with GDP. *J. Mol. Biol. 217*, 503−516.

(29) Ito, Y., Yamasaki, K., Iwahara, J., Terada, T., Kamiya, A., Shirouzu, M., Muto, Y., Kawai, G., Yokoyama, S., Laue, E. D., Walchli, M., Shibata, T., Nishimura, S., and Miyazawa, T. (1997) Regional polysterism in the GTP-bound form of the human c-Ha-Ras protein. *Biochemistry 36*, 9109−9119.

(30) Saris, N. E., Mervaala, E., Karppanen, H., Khawaja, J. A., and Lewenstam, A. (2000) Magnesium. An update on physiological, clinical and analytical aspects. *Clin. Chim. Acta 294*, 1−26.

(31) Kretsinger, R. H. (1976) Calcium-binding proteins. *Annu. Rev. Biochem. 45*, 239−266.

(32) Buhrman, G., O'Connor, C., Zerbe, B., Kearney, B. M., Napoleon, R., Kovrigina, E. A., Vajda, S., Kozakov, D., Kovrigin, E. L., and Mattos, C. (2011) Analysis of binding site hot spots on the surface of Ras GTPase. *J. Mol. Biol. 413*, 773−789.

(33) Maurer, T., Garrenton, L. S., Oh, A., Pitts, K., Anderson, D. J., Skelton, N. J., Fauber, B. P., Pan, B., Malek, S., Stokoe, D., Ludlam, M. J. C., Bowman, K. K., Wu, J., Giannetti, A. M., Starovasnik, M. A., Mellman, I., Jackson, P. K., Rudolph, J., Wang, W., and Fang, G. (2012) Small-molecule ligands bind to a distinct pocket in Ras and inhibit SOS-mediated nucleotide exchange activity. *Proc. Natl. Acad. Sci. U.S.A. 109*, 5299−5304.

(34) Brenke, R., Kozakov, D., Chuang, G. Y., Beglov, D., Hall, D., Landon, M. R., Mattos, C., and Vajda, S. (2009) Fragment-based

identification of druggable 'hot spots' of proteins using Fourier domain correlation techniques. *Bioinformatics 25*, 621−627.
(35) Rosnizeck, I. C., Graf, T., Spoerner, M., Trankle, J., Filchtinski, D., Herrmann, C., Gremer, L., Vetter, I. R., Wittinghofer, A., Konig, B., and Kalbitzer, H. R. (2010) Stabilizing a Weak Binding State for Effectors in the Human Ras Protein by Cyclen Complexes. *Angew. Chem., Int. Ed. 49*, 3830−3833.
(36) Barbacid, M. (1987) ras Genes. *Annu. Rev. Biochem. 56*, 779−827.
(37) Murray, D., Ben-Tal, N., Honig, B., and McLaughlin, S. (1997) Electrostatic interaction of myristoylated proteins with membranes: Simple physics, complicated biology. *Structure 5*, 985−989.
(38) Kholodenko, B. N., Hoek, J. B., and Westerhoff, H. V. (2000) Why cytoplasmic signalling proteins should be recruited to cell membranes. *Trends Cell Biol. 10*, 173−178.